Oocytes Could Rearrange Immunoglobulin Production to Survive over Adverse Environmental Stimuli

Yang Wang
Nanjing Medical University
Fu-Qiang Luo
Nanjing Medical University
Yu-Hao He
Nanjing Medical University
Zhi-Xia Yang
Nanjing Medical University
Xin Wang
Nanjing Medical University
Cong-Rong Li
Nanjing Medical University
Bei-Qi Cai
Sir Run Run Hospital Nanjing Medical University
Liang-Jian Chen
Nanjing Medical University
Zi-Bin Wang
Nanjing Medical University
Yi-Chun Guan
Zhengzhou University Third Hospital and Henan Province Women and Children's Hospital
Cui-Lian Zhang
Henan Provincial People's Hospital
dong Zhang (dong.ray.zhang@njmu.edu.cn)
Nanjing Medical University https://orcid.org/0000-0002-0257-4441

Research Article

Keywords: Oocytes, Immunoglobulin, Environmental Stimuli

Posted Date: April 11th, 2022

DOI: https://doi.org/10.21203/rs.3.rs-1454648/v1

Abstract

Immunoglobulins are key humoral immune molecules produced and secreted by B lymphocytes at various stages of differentiation. No research has reported whether immunoglobulins are present in the non-proliferative female germ cells—oocytes—and whether they are functionally important for the quality, self-protection, and survival of oocytes. Herein, we found that IgG was present even in the oocytes of immunodeficient mice; the IgG-VDJ regions were highly variable between different oocytes, and H3K27Ac bound and regulated IgG promoter region. Next, IgG mRNA and protein levels increased in response to LPS, and this increment required CR2 on the oocyte membrane. Finally, we revealed three aspects of the functional relevance of oocyte IgG: first, oocytes could upregulate IgG to counteract the increased ROS level induced by CSF1; second, oocytes could upregulate IgG in response to injected virus ssRNA to maintain mitochondria integrity; third, upon bacterial infection, oocytes could secret IgG out to encompass bacteria to survive better than other somatic cells. This study reveals for the first time that the female germ cells, oocytes, can independently adjust intrinsic IgG production to survive in adverse environments.

Introduction

Immunoglobulins are key humoral immune molecules produced and secreted by B lymphocytes at various stages of differentiation. Another unique feature of immunoglobulins is that in reaction to immunogens, immunoglobulin genes always rearrange before transcription, leading to their extreme polymorphism (1, 2). Several proteins, such as CTCF (3), RAG1/2 (4, 5), VprBP (6), and NF-kappa B (7), are all essential in the rearrangement. Although immunoglobulins have recently been found to exist in several other types of normal cells, including sperm (8), islet cells (9), hepatocytes (10), umbilical cord endothelial cells (11), and eye cells (12), the functional relevance of IgG is far from clearly understood.

Mammalian oocytes are quite distinct from B lymphocytes in several respects. Each diploid Oocyte goes through meiosis to produce three degenerating haploid polar bodies and one haploid mature oocyte, which do not continue to go through mitosis or meiosis; mature oocytes, although not proliferative, can mate with a sperm to resume their capacity for division and regenerate stem cells that can differentiate into any tissue cell; oocytes store plenty of maternal RNAs and proteins and before resuming meiosis, are transcriptionally quiescent. The oocyte is thought to be a non-professional phagocyte because the fertilization process is somehow similar to phagocytosis, and there are phagocytosis-promoting receptors on the oocyte membrane, including FcγR, CR-1, CR-3, and C1q-R (13). However, no study has shown that oocytes can perform like B lymphocytes to rearrange and produce immunoglobulin.

However, our previous transcriptome and proteome data on mouse oocytes frequently detected immunoglobulin mRNA or protein fragments, prompting us to speculate that oocytes could transcribe and translate immunoglobulin genes. In the present study, we not only prove that immunoglobulin mRNA and protein do exist in the oocytes, we also find that oocytes can rearrange immunoglobulin production to survive over adverse environmental stimuli.

Results

Immunoglobulins are present in oocytes and increase in response to environmental immunogens

Previous studies have found that immunoglobulins also exist within sperm (8), islet cells (9), hepatocytes (10), umbilical cord endothelial cells (11) and eye cells (12) except within B cells. However, the biological relevance of the immunoglobulin within these non-B cells is not known. Oocytes are a special type of terminally differentiated cells that are physically well-protected from viruses or bacteria because they are surrounded by granular cells and embedded inside ovaries. However, oocytes can be damaged by some extremely adverse conditions, such as severe sepsis (14), severe salpingitis (15), and a cytokine storm during a virus infection (16). Furthermore, in-vitro maturation or fertilization greatly increase the risk of oocyte being harmed by an adverse cultural environment, such as a contaminated mineral oil or medium. Thus, if oocytes had the capacity to produce immunoglobulin and increase its expression in response to environmental immunogens, they could have a greater chance of survival than other somatic cells. Moreover, we frequently saw the presence of immunoglobulin mRNA or protein fragments in ovary transcriptomic or proteomic sequencing databases.

We firstly examined the presence of IgG, IgA, and IgM in the oocytes through immunostaining and Western blot. We did see the obvious presence of these immunoglobulins within oocytes (Fig. 1A). Immunoprecipitation using the IgG antibody within oocyte lysate, SDS-PAGE, silver staining, and LCMS successfully identified IgG fragments (Fig. 1B, blue-highlighted line in suppl. dataset 1). Because IgG is the major type of immunoglobulin, we focused on IgG. However, no IgG was seen in granular cells or somatic NIH3T3 cells (Fig. 1C-E). Finally, we examined IgG levels in immunoglobulin-deficient SCID (severe combined immune-deficiency) mice and didn't detect any IgG within their serum (Fig. 1F and 1G); however, SCID oocytes had a level of IgG similar to that of control oocytes (Fig. 1H-J). Finally, immuno-EM further verified the presence of IgG within diverse cytoplasmic organelles such as vesicle (Fig. 1K) and mitochondria (Fig. 1L). These results suggest that immunoglobulin did exist in oocytes independently of the overall immune system.

Generally, the IgG level increases in B lymphocytes in response to pathogens. We examined whether this could also occur in oocytes. We first used LPS, a common pathogen from gram-negative bacteria, to treat oocytes. Immunostaining and blotting both showed that the IgG level was significantly raised in the LPS-treated oocytes (Fig. 2A-D), whereas neither the LPS-treated granular cells (GCs, Fig. 2E and 2F) nor the NIH3T3 (3T3, Fig. 2G and 2H) cells showed any increment in IgG levels. Moreover, p-NFKB (p-p65) also significantly increased with LPS stimuli (Fig. 2I and 2J).

These results suggested that immunoglobulins are present in mouse oocytes independently of the overall immune system, and that oocytes could rearrange IgG production in response to environmental stimuli.

Membrane receptor CR2 mediates IgG production in response to environmental LPS

In lymphocytes, beside through TLRs (Toll-like receptor) (17–20), the transduction of extrinsic immunogenic signal in the cells can also be mediated through several other types of receptors such as CD46 (CD46 antigen, complement regulatory protein) (21), FCGR1A (Fc fragment of IgG receptor Ia) (22) and CR2 (complement receptor 2) (23). Interestingly, these receptors are present within the oocyte membrane (13). Therefore, we wanted to know which mediated the IgG production in response to immunogenic extrinsic LPS.

We found that on exposure to LPS stimuli, the IgG level significantly increased by one fold, while CD46 blockage with the anti-CD46 antibody had no impact on the IgG increment on exposure to LPS stimuli (Fig. 3A and 3B). Similarly, FCGR1A blockage with the anti-FCGR1A antibody had no impact on the IgG increment on exposure to LPS stimuli (Fig. 3C and 3D). In contrast, CR2 blockage with the anti-CR2 antibody largely counteracted the IgG increment on exposure to LPS stimuli (Fig. 3E and 3F).

The NFKB pathway played an essential role in regulating IgG production inside the lymphocytes (24, 25), Next, we wanted to know whether this was also true for oocytes. We found that CR2 blockage with the anti-CR2 antibody also largely counteracted the p-p65 increment on exposure to LPS stimuli (Fig. 3G and 3H), while inhibition of the NFKB pathway with a specific inhibitor SC75741 (Fig. 3I and 3J) largely counteracted the IgG increment on exposure to LPS stimuli (Fig. 3K and 3L).

These results suggested that membrane CR2 is essential for IgG increment on exposure to LPS stimuli, whereas NFKB is also essential inside the oocytes, probably because it receives the activation upstream signal from CR2 (Fig. 3M).

IgG transcription increased and was regulated by H3K27ac on exposure to CSF1 or LPS stimuli

Generally, from the perspective of IgG genes, B cells are distinct from each other; Highly-variable regions, comprising hundreds of V, D, and J genes, undergo pre-setup recombination for each specific potential immunogen. On exposure to a certain immunogen stimulation, a B cell having a corresponding recombined VDJ type is awakened and clones itself into a colony of B cells having the same VDJ type. Oocytes have IgG even in the absence of environmental immunogen stimulation, and they increase IgG production on exposure to stimulation. Therefore, we are interested to know whether oocytes are distinct from each other in terms of IgG VDJ regions without immunogen stimulation, and whether the VDJ region undergoes recombination again on exposure to stimulation.

First, we found that IgG mRNA, as indicated by the PCR product of IgG VDJ region, existed in oocytes (Fig. 4A) without immunogen stimulation; moreover, sequencing showed that the VDJ region was distinct between randomly-examined individual oocytes (Fig. 4B). Next, we found that gross IgG-constant mRNA increased on exposure to CSF1 or LPS stimuli (Fig. 4C and 4D).

Post-translation modified histones, for example, H3K4me^3 and H3K27ac (26), have been confirmed to bind to the upstream regulating sequences to promote IgG transcription. We wanted to see whether the histones regulate, and which histones, regulate IgG transcription. Chip-seq showed that on exposure to either LPS or CSF1 stimuli, H3K27ac decreased its binding to the regulating sequences of all genes (Fig. 4E); however, its binding to the regulating sequences of the IgG gene significantly increased (Fig. 4F). In contrast, H3K4 showd decreased binding on exposure to LPS or CSF1 stimuli (Suppl. Figure 1).

IgG functions to eliminate ROS production in response to environmental stimuli

It appeared that oocytes perform like immune cells to adjust IgG production. Next, we wanted to see whether IgG is functionally important for the maintenance of quality and survival of the oocyte itself.

We first examined the relationship between the IgG level and the ROS level, which is essential for cell quality (27). We found that on exposure to CSF1 stimuli, the IgG level significantly decreased by approximately one fold (Fig. 5A and 5B), whereas the ROS level also decreased (Fig. 5C and 5D). In contrast, the H2O2 treatment significantly elevated the ROS level, whereas the CSF1 treatment pulled the H2O2-induced ROS level back to the control level (Fig. 5C and 5D). Next, co-treating CSF1-stimulated oocytes with NMN, a well-known ROS remover, pulled the CSF1-induced IgG level back to the control level (Fig. 5A and 5B), and CSF1/NMN co-treated oocytes had significantly higher ROS levels than NMN-treated oocytes. These phenomena led us to presume that CSF1 stimulation could increase both ROS and IgG protein level, whereas increased IgG act as an endogenous anti-oxidant to counteract excessive toxic ROS (Fig. 5E). In further support, IgG inhibition counteracted the CSF1-induced decrease in ROS, whereas IgG inhibition counteracted the ROS decrement caused by co-treating H2O2-challeging oocytes with CSF1 (Fig. 5F and 5G).

In summary, all the evidences supported that IgG could be utilized to reduce the superfluous detrimental ROS induced by enviromental stimuli, such as CSF1 challenge (Fig. 5H).

IgG functions to protect mitochondria integrity in response to virus ssRNA stimuli

Virus ssRNA (single-strand RNA) has been shown to elicit the inflammation and immune response of host cells (28). Next, we examined how IgG functions in response to virus ssRNA. We used a mixture of two GU-rich ssRNA to mimic virus RNA as reported (29). We found that ssRNA injection significantly increased IgG level (Fig. 6A-D), while inhibition of the NFKB pathway pulled ssRNA-elevated IgG back to near the control level (Fig. 6C and 6D). Furthermore, ssRNA injection significantly increased the p-p65 level, which was also able to be pulled back to control by SC75741 (Fig. 6E and 6F).

Next, we found that both ssRNA injection and NFKB inhibition caused increased mitochondria aggregation, accordingly ATP level significantly decreased upon either treatment. While ssRNA injection

combined with NFKB inhibition further exacerbate mitochondria aggregation, accordingly ATP level further decreased. (Fig. 6G and 6H).

Finally, we found that the early apoptotic level as indicated by Annexin V, significantly increased upon ssRNA injection combined with NFKB inhibition (Fig. 6I and 6J).

These results indicated that virus ssRNA-induced, NFKB-mediated IgG increment could protect mitochondria integrity from ssRNA-induced inflammation.

IgG functions to promote oocyte survival in response to E. coli stimuli

Although oocytes are normally embedded within the ovaries and protected from environmental infection, they could be impacted by severe physical infection such as severe sepsis (14), severe salpingitis (15), or a cytokine storm during virus infection (16). Therefore, we next wanted to determine whether IgG is active during infection, and how it functions.

We first found that IgG-constant mRNA significantly increased on exposure to E. coli stimuli (Fig. 7A and 7B), whereas the Western blot showed that IgG protein levels significantly decreased (Fig. 7C and 7D). Then, immunofluorescence also showed that on exposure to E. coli stimuli, IgG intensity within oocytes significantly decreased (Fig. 7E and 7F), however, the membrane/cytoplasm IgG ratio significantly increased (Fig. 7E and 7G). Next, we injected cy2-conjugated donkey anti-mouse IgG into the oocytes and tracked the dynamics of IgG. Live imaging showed that after two hours of E. coli stimuli, large IgG aggregates gradually increased across the whole membrane, from the inner side to outer side (Fig. 7H and 7I), indicating that on exposure to E. coli stimuli, IgG could aggregate onto the membrane and then be secreted out of the oocytes. However, we did not see the bright IgG dots at the outside of the zona pellucida (ZP), probably due to the quick disassembly of the IgG aggregates once they were secreted out of the ZP. However, oocyte-treating E. coli showed significantly increased IgG (Fig. 7J-L), suggesting that excreted IgG could encompass and precipitate E. coli.

Next, we examined how the increased IgG would be beneficial for E. coli-challenged oocytes. In-vitro maturation (IVM) results showed that E. coli- challenged oocytes had a 23.23% decreased maturation rate compared with control oocytes (Fig. 7M and 7N, rate of 1pb, first polar body, E. coli-challenged vs. control, 71.65% vs. 55%); In contrast, the E. coli-challenging of NIH3T3 cells reduced their mitotic indexes from 5.52–2.35% (Fig. 7O). Apparently, the extent of maturation decrement of oocytes was much smaller than that of NIH3T3 cells upon E.coli challenge (Fig. 7P). However, oocytes co-treated with IgG-inhibition and E-coli caused more than a fold decreased maturation rate (Fig. 7M and 7N, rate of 1pb, E. coli plus IgG inhibition vs. control, 71.65% vs. 34%).

Finally, although their maturation rate was decreased on exposure to E. coli treatment, the maturated MII oocytes had normal chromosome alignment; however, IgG inhibition together with E. coli treatment

significantly increased the percentage of oocytes with abnormal chromosome alignment (Fig. 7Q and 7R).

These results suggested that oocytes could increase IgG production to survive over bacterial infection.

Discussion

In the present study, we not only found that immunoglobulins exist within mouse oocytes, but also verified that IgG was important for the self-protection and quality maintenance of oocytes in response to environmental stimuli. Furthermore, we also uncovered how immunoglobulin level was regulated.

Immunoglobulins are key humoral immune molecules produced and secreted by B lymphocytes at various stages of differentiation. However, several other types of cells, such as sperm (8), islet cells (9), hepatocytes (10), umbilical cord endothelial cells (11) and eye cells (12) were also reported to contain immunoglobulins. However, these studies only showed some of the functional relevance of IgG in these cells. In the present study, through a logical experimental series design, we uncovered at least three aspects of the important biological function of oocyte IgG, which support that oocyte IgG could exert similar immune function to lymphocytes. Moreover, we also found both similarities and differences about the ways ocyte IgG function.

In terms of IgG structure, rearrangement of the VDJ region can occur even before stimuli in both cells, and the VDJ region of individual cells were distinct from each other. However, in the western blot test, the molecular size of the oocyte IgG heavy chain was about 70 KDa, whereas lymphocyte IgG heavy chain was about 55 KDa, thus oocyte IgG is more like IgY. Moreover, the oocyte IgG level remained unchanged in the SCID mice, suggesting that oocyte IgG was independent of the overall immune system, and oocyte IgG could protect itself even under conditions of systemic immunodeficiency, which agree with the observation that HIV patients can have normal fertilization and early embryo development.

For the upstream signal pathway that regulates IgG level, NFKB is the essential mediator that receives signals from the membrane and enters the nucleus to regulate *IgG* transcription for both oocytes and lymphocytes. However, oocytes appeared to receive signals from external stimuli mainly through CR2 instead of CD46 or FCGR1A, although all of these receptors sense outer stimuli in lymphocytes.

For the epigenetic regulation of the *IgG* gene, modified histone can regulate IgG transcription in both oocytes and lymphocytes (26). However, in oocytes, H3K27ac showed positive binding, while H3K4 showed negative binding onto IgG regulating sequences on exposure to both CSF1 and LPS stimuli, whereas in lymphocytes, H3K4me3 showed positive binding onto IgG regulating sequences (26).

Overall, in the present study, we found that the oocyte could rearrange IgG production to protect itself from adverse environmental stimuli. Although the mechanism is partially different from that of lymphocytes, oocytes behave like immune cells. However, because the oocyte cannot reproduce itself, the

IgG might only be used for self-protection. Further investigation is required to uncover more detailed mechanisms and the functional relevance of oocyte IgG.

Materials And Methods

Mice

Animal experimental procedures in our study were all approved by the Animal Ethics Committee of Nanjing Medical University (NJMU) (approval no. IACUC-1809011), and all mice were housed in the Animal Core Facility (ACF) of NJMU under standard specific pathogen free (SPF) conditions of ACF.

Three-week-old SCID (Severe Combined Immunodeficient) mice were bought from Beijing Vital River Laboratory Animal Technology Co., Ltd. (Beijing, China) and housed in the ACF.

Three-week-old control CD1/ICR mice were bought from ACF.

Antibodies

Primary antibodies: Anti Beta Actin mAb (Cat#:S6007M, Bioworld, Dublin, OH, USA); Rabbit anti OMPC (Cat#: bs20213R, Bioss Antibodies, Beijin, China); Acetyl-Histone H3(K27)(D5E4) XP(R) rabbit mAb (Cat#: 8173s, Cell Signaling Technology, Danvers, MA, USA); Histone H3 (Trl-Methyl K4) pAb (Cat#: BS7232, Bioworld, Dublin, OH, USA); CR2 rabbit pAb (Cat#: A8407, ABclonal, Wuhan, Hubei, China); CD46 rabbit pAb(Cat#: A1653, ABclonal, Wuhan, Hubei, China); FCGR1A pAb (Cat#: BS6238, Bioworld, Dublin, OH, USA); Phospho-Histone H3(Ser 10) Mouse McAb (Cat#: 66863-1-Ig; Proteintech, Rosemont, IL, USA); Tubulin α (G436) mAb (Cat#: BS1699M; Bioworld, Dublin, OH, USA); Anti-RELA (Phospho-Ser536) rabbit polyclonal antibody (Cat#: D155006; BBI, Shanghai, China), AffiniPure Goat anti-Mouse IgG, light chain specific (Jackson ImmunoResearch Laboratory, Cat#: 115-005-174, West Grove, PA, USA).

Secondary antibodies: Horseradish peroxidase (HRP)-conjugated rabbit anti-goat IgG and HRP-conjugated goat anti-mouse IgG were purchased from Jackson ImmunoResearch Laboratory (West Grove, PA, USA). Goat anti-mouse IgA-FITC (Bersee, Cat#: BFR522, Beijing, China); Goat anti-mouse IgM-FITC (Bersee, Cat#: BFR523, Beijing, China); Cy2-conjugated donkey anti-mouse IgG (Code: 715-225-150), Cy3-conjugated donkey anti-mouse IgG (Code: 715-165-150), all purchased from Jackson ImmunoResearch Laboratory (West Grove, PA, USA).

Oocyte Collection and In Vitro Culture

Fully-grown GV oocytes were collected from three-week-old female control or SCID mice. Oocytes were released by puncturing follicles with a sterile syringe needle in a MEM+ medium (0.01 mM EDTA, 0.23 mM Na-pyruvate, 0.2 mM penicillin/streptomycin and 3 mg/ml BSA in MEM). After the cumulus cells from the cumulus-oocyte complexes (COC) were washed off, cumulus-free oocytes were cultured in 100 μl mini-drops of MEM+ containing 10% fetal bovine serum (FBS) (Thermo Fisher) covered with mineral oil at 37.0 °C in an incubator with 5% O_2, 5% CO_2, and a humidified atmosphere.

Cell Culture and mitotic index assay

NIH3T3 cells were from ATCC (Cat No.: CRL-1658) and sold by Procell Life Science & Technology Co. (Wuhan, Hubei, China). The cells were cultured in DMEM with 10% FBS. For mitotic index assay, NIH3T3 cells were fixed and immunostained for tubulin and p-H3, the cells with strong p-H3 staining on the chromosomes are mitotic cells. For each sample, at least 1000 cells were counted. Mitotic index is the number of mitotic cells divided by the number of total counted cells.

Immunofluorescence Staining of Oocytes and Image Taking

Two distinct protocals were used for the permeation & fixation of oocytes. The blocking, primary antibody incubation, secondary antibody incubation and oocyte mounting procedures after permeation & fixation are the same for these two protocals.

Permeation & fixation

1). For experiments in Fig. 7E-G, we wanted to maintain IgG signals furthest on the membrane. After three times of quick wash in PBS/0.05% PVP (polyvinylpyrrolidone), oocytes were first fixed in 3.7% FPA in PHEM for 30 minutes at room temperature and washed with PBS/PVP three times at 10 minutes each. Then oocytes were permeated in 1% Triton X-100/PHEM (60 mM PIPES, 25 mM Hepes, pH 6.9, 10 mM EGTA, 8 mM $MgSO_4$) for 10 minutes.

2). For all other experiments except Fig. 7E-G, we wanted to get best quality of cytoplasmic signal. After three times of quick wash in PBS/PVP, oocytes were first permeabilized with 0.5 % Triton X-100/PHEM (60 mM PIPES, 25 mM Hepes, pH 6.9, 10 mM EGTA, 8 mM $MgSO_4$) for 5 minutes. After washed with PBS/PVP three times at 10 minutes each, oocytes were fixed in 3.7% FPA in PHEM for 20 minutes at room temperature.

Blocking, primary antibody incubation, secondary antibody incubation and oocyte mounting:

After being washed with PBS/0.05% PVP (polyvinylpyrrolidone) three times at 10 minutes each, oocytes were blocked in blocking buffer (100 mM glycine and 1% BSA in PBS) for one hour at room temperature. Primary antibodies were then diluted in blocking buffer and oocytes were incubated in it overnight at 4.0 °C. Fluorescent secondary antibodies (Jackson ImmunoResearch Laboratories) were used at 7.5 μg / ml. DNA was stained with 0.3 μg / ml Hoechst 33258. Next, buffers were were slowly and gently removed from around the oocytes, which immobilized the oocytes on the slide; then a drop (about 5-10 μl) of anti-fade solution (0.25% n-propyl gallate and 90% glycerol in PBS) was mounted onto the oocytes and oocytes were covered by a coverglass. To avoid the deformation of the oocytes, a double-stick tap was pre-placed between the slides and coverslips. Specimens were imaged with IQ2 on an Andor Revolution spinning-disk confocal system (Andor Technology PLC, Belfast, UK) mounted on an inverted TiE microscope (Nikon, Japan) with a 60 ×, 1.4 NA objective and captured with cold CCD camera (Andor). Most images are displayed as maximum intensity projections of the captured z stacks.

Immunoprecipitaion, commassie staining and mass-spec

2.5 μg HRP-conjugated goat anti-mouse IgG antibody was first coupled to 30 μl protein-A/G beads (Yeasen, Shanghai, China) for 4 hours at 4°C on a rotating wheel in 250 μl immunoprecipitate (IP) buffer (20 mM Tris-HCl, pH 8.0, 10 mM EDTA, 1 mM EGTA, 150 mM NaCl, 0.05% Triton X-100, 0.05% Nonidet P-40, 1 mM phenylmethylsulfonyl fluoride) with 1:100 protease inhibitor (Sigma) and 1:500 phosphatase inhibitor (Sigma). Meanwhile, 400 oocytes were lysed and ultrasonicated in 250 μl IP buffer and then pre-cleaned with 30 μl protein-A/G beads for 4 hours at 4 °C. After that, protein A/G-coupled Rabbit IgG or specific antibody were incubated overnight at 4 °C with pre-cleaned oocyte lysate supernatant. Finally, after being washed three times (10 minutes each with 250 μl IP buffer), the resulting beads with bound immunocomplexes were subjected to SDS-PAGE and commassie staining. The gel band corresponding to the band from IgG blot was cut out and sent to Biotech-pack (Beijing, China) for mass spec identification of proteins.

CHIP-seq

H3K27ac and H3K4me3 CHIP-seq were perform with Hyperactive In-Situ ChIP Library Prep Kit under Targets and Tagmentation (CUT&Tag) technology (Vazyme) according the manufacturer's instruction. The kit using a hyperactive Tn5 transposase to precisely binds the DNA sequence near the target protein. In brief, lysate of 100 oocyte were incubated with ConA beads, then primary and secondary antibody were in turn incubated with oocyte lysate, next Hyperactive pG-Tn5/pA-Tn5 Transposon was incubated with the sample and tagmentation were performed. Finally DNA was extracted and library was prepared as instructed, and DNA library was sent to Novogene (Beijing, China) for sequencing.

Virus SSRNA production and microinjection

Immunity-inducing GU-rich virus ssRNA (Single-strand RNA) sequences were according to reported (25). We selected two sequences: 5'-GACTTGAGCGAGCGCTTTTTT-3' (ssRNA-6T) and 5'-GTCCGGGCAGGTCTACTTTTT-3' (ssRNA-5T). SsRNA were produced and purified using the T7 Ribomax Express RNAi System (Promega) according to the manufacturer’s instructions, then aliquoted and stored at -80°C. The difference here is that the RNA is single-stranded from one transcription reaction. Primers for DNA templates are in suppl. table 2.

SsRNA was adjusted to 5uM with nuclease-free water, and about 10 pl of ssRNA was injected into GV oocytes with a programmed microinjector. 10 μM milrinone was included to prevent GVBD.

LPS, CSF1, H2O2, NMN and SC75741 treatment

LPS (Cat#: L2880, Sigma, St. Louis, MO, USA) was added into oocyte IVM medium at a final conc. of 10 EU/ml for 16 hour; CSF1 (Cat#: HZ-1207, Proteintech, Rosemont, IL, USA) was added into oocyte IVM medium at a final conc. of 10 ng/ml for 16 hour; H2O2 (Cat#: 88597, Sigma, St. Louis, MO, USA) was added into oocyte IVM medium at a final conc. of 30 mM for 30 min; NMN (Cat#: S5259, Selleck Chemicals, Houston, TX, USA) was added into oocyte IVM medium at a final conc. of 1 mM for 16 hour;

SC75741 (Cat#: S7273, Selleck Chemicals, Houston, TX, USA) was added into oocyte IVM medium at a final conc. of 0.1 μM for 16 hour.

E-coli fluorecence labeling and treating oocytes with E-coli

FICT-d-Lys（Cat#: I0201,Bioluminor, XiaMen, Fujian, China）was added into LB medium at a final conc. of 0.1mM. 2.5 μl DH5α competent E.coli (Cat#: C502, Vazyme, Nanjing, Jiangsu, China) were added into 1 ml LB medium and the E.coli culture were grown at 37 °C until OD600 reached 0.6. Then E.coli was collected and washed by PBS, then re-suspend 1ml PBS. Finally, 10 μl PBS / with Ecoli was added into 100 μl IVM medium with 50 oocytes during the whole IVM period. Except for maturation assay done at 16 hour of E.coli treatment, all other E.coli-treated oocyte experiment were done at 6 hour.

Antibody inhibition

Antibodies for CR2, CD46 and FCG1R were added into oocyte IVM medium at a final conc. of 0.05 mg/ml to inhibit corresponding receptor on the oocyte membrane. 0.065 mg/ml antibody for IgG light chain was microinjected into GV oocytes (10m pl per oocyte) to inhibit IgG. To remove the toxic preservative within the commercial antibodies, the antibodies were buffer-exchanged into PBS/50% glycerol with a size-exclusion spin column until the original preservative-containing antibody solution was less than 10^{-4} of the final solution.

Oocyte cDNA Synthesis and Amplification of IgG VDJ region

RNA extraction and cDNA synthesis were performed with NEBNext® Single Cell/Low Input cDNA Synthesis& Amplification Module (Cat No.: E6421, NEB, Lpswich, MA, USA) according to the instruction from 100 oocytes. For IgG VDJ amplification, two round of PCR were done with two set of primers respectively. The primer sequences are in supplementary table 1. The DNA polymerase was Phanta high-fidelity DNA polymerase (Cat No.: P505-d1, Vazyme, Nanjing, Jiangsu, China). Then PCR products were ligated into cloning vector (Vazyme, Cat No.: C601-02) and transformed into competent DH5α, and 50 colonies (ligated cDNA from each colony corresponds to the mRNA of a single oocyte) were sent to GENEWIZ (Suzhou, Jiangsu, China) for sequencing.

Detection of ROS Generation

The ROS Assay Kit (Cat#: S0033, Beyotime, Beijing, China) was used to detect ROS generation in oocytes. In brief, oocytes were incubated with a dichlorofluorescein diacetate (DCFH-DA) probe for 20 min at 37 °C in the dark, washed, and mounted on slides for confocal imaging.

Mitochondrial staining and ATP measurements

For mitochondrial staining, oocytes were incubated in Hepes containing 100 nM Mito Tracker (Cat#: M7521, Invitrogen, Carlsbad, CA, USA) and 10 μg/ml Hochest 33342 (Sigma) for 30 min. Images were taken with an Andor Revolution spin disk confocal workstation.

For ATP measurements, 15 oocytes were first lysed with 100 μl ATP lysis solution (Cat#: S0026, Beyotime) on ice. The samples were then detected by enzyme-labeled instrument Synergy2 (BioTek, Winooski, VT, USA) to evaluate ATP level.

Apoptosis detection

Apoptosis was detected with an Annexin V-FITC/PI Apoptosis Detection Kit (Cat#: 40302ES20, YEASEN). Oocytes were stained with 5 μl annexin V-FITC and 10 μL PI Staining Solution diluted in 100 μl binding buffer for 15 min in the dark at RT. After washing, oocytes were mounted onto glass slides, and images were obtained as above.

Animal / oocyte inclusion, experiment grouping, data collection, and data analysis

Any selected oocyte must be of normal quality (fully-grown oocyte from an antral follicle, normal diameter, tight connection between zona pellucida and oocyte membrane, etc). Any selected female mouse has to be physically healthy (normal body weight, eats normally, normal activity, etc). Any oocyte or mouse of bad quality or unhealthy will be excluded.

For sample size in oocyte-related experiment, about 3-5 oocytes were randomly selected for one repeat and thus about 9-15 oocytes were analyzed for three independent repeats. We found that measurements from 9-15 oocytes could form a normal distribution and are fairly reliable for a statistic analysis. For sample size in mouse-related experiment, similarly, about 3-5 mice were randomly selected for one repeat and 9-15 mice were analyzed for three independent repeats.

We tried to follow the double-blinding roles for both mouse and oocyte-related experiment grouping, data collection, and data analysis. For each independent repeat, oocytes were obtained from multiple mice to eliminate natural differences between individuals; oocytes were randomly divided into different experimental groups. About 50 oocytes per group for immunofluorescence / live fluorescence or 100 oocytes per group for western blot were used. For image taking, the order for different groups was solely random. And within the same group, oocytes were again randomly selected for image taking (We didn't take images from all oocytes). The index setting for image taking was always identical for each group of the same experiments. The order of different groups for data measurement is also random. All intensity measurements were done with Image J on the original tif file without any adjustment of brightness/contrast. Fluorescence intensity was always a net intensity obtained by a measured image intensity subtracted by the adjacent background intensity. For band quantification in western blot, an integrated intensity was obtained by the average intensity multiplied by the band area; the average intensity was again obtained by measured image intensity subtracted by the adjacent background intensity.

Statistical Analysis

All experiments were repeated at least three times. Data are presented as mean ± SEM. Comparisons between two groups were made by Student’s t test. Differences among more than two groups were

compared using one-way ANOVA. $P < 0.05$ was considered statistically significant. Statistical analyses were conducted with GraphPad Prism.

Abbreviations

CTCF: CCCTC-binding factor
RAG1/2: Recombination activating gene 1/2

VprBP: DDB1 and CUL4 associated factor 1

NF-kappa B: v-rel reticuloendotheliosis viral oncogene homolog A, also known as NFKB, p65

FcγR: Fc receptor

CR-1: complement receptor 2, also known as CR2

CR-3: integrin alpha M

C1q-R: CD93 antigen

LCMS: Liquid Chromatography Mass Spectrometry

SCID: server combined immune-deficiency

LPS: Lipopolysaccharide

GCs: granular cells

CD46: CD46 antigen, complement regulatory protein

FCGR1A: Fc fragment of IgG receptor Ia

CSF1: colony stimulating factor 1

NMN: Nicotinamide mononucleotide

ssRNA: Single-Stranded Ribonucleic Acid

ZP: zona pellucida

IVM: In-vitro maturation

HIV: human immunodeficiency virus

Declarations

Acknowledgement

We thank Professor Shuo Yang and Professor Xiao-Ming Wang from Department of Immunology, Nanjing Medical University, and Wei-Guo Zhang from Suzhou Institute of Systematic Medicine, Systematic Medical Research Center, Chinese Academy of Medical Sciences for valuable advices.

competing interests

The authors declare that they have no competing interests.

Author contributions

Dong Zhang, Cui-Lian Zhang, Yi-Chun Guan and Zhi-Xia Yang designed the research. Yang Wang, Fu-Qiang Luo and Yu-Hao He performed most of the experiments. Xin Wang, Cong-Rong Li, Bei-Qi Cai, Liang-Jian Chen and Zi-Bin Wang assisted during the experiments. Yang Wang did all data analysis and prepared figures under the direction of Dong Zhang, Cui-Lian Zhang, Yi-Chun Guan and Zhi-Xia Yang. Dong Zhang and Zhi-Xia Yang wrote the manuscript, Cui-Lian Zhang and Yi-Chun Guan proofread and gave advice.

Funding

This work is financially supported by the General Program of the National Natural Science Foundation of China (Grant No: 32070840) to Dong Zhang, the major project of Henan Provincial medical science and technology plan (Grant No. SBGJ202001002) to Cui-Lian Zhang and Science and technology research plan of Henan Province (Grant No. 202102310061) to Yi-Chun Guan.

data Availability

The data that support the findings of this study are available from the corresponding author upon reasonable request. Chip-seq raw data have been deposited into GEO repository, the accession No. is GSE191278. Supplementary Dataset 1 has been deposited into Zenodo, the DOI is 10.5281/zenodo.5793909.

References

1. Tolar P. Cytoskeletal control of B cell responses to antigens. Nat Rev Immunol. 2017 Oct;17(10):621–634. doi: 10.1038/nri.2017.67. Epub 2017 Jul 10. PMID: 28690317.
2. de Villartay JP, Fischer A, Durandy A. The mechanisms of immune diversification and their disorders. Nat Rev Immunol. 2003 Dec;3(12):962 – 72. doi: 10.1038/nri1247. PMID: 14647478.
3. Ribeiro de Almeida C, Stadhouders R, de Bruijn MJ, Bergen IM, Thongjuea S, Lenhard B, van Ijcken W, Grosveld F, Galjart N, Soler E, Hendriks RW. The DNA-binding protein CTCF limits proximal Vkappa recombination and restricts kappa enhancer interactions to the immunoglobulin kappa light chain locus. Immunity. 2011 Oct 28;35(4):501 – 13. doi: 10.1016/j.immuni.2011.07.014.

4. Mombaerts P, Iacomini J, Johnson RS, Herrup K, Tonegawa S, Papaioannou VE. RAG-1-deficient mice have no mature B and T lymphocytes. Cell. 1992 Mar 6;68(5):869 – 77. doi: 10.1016/0092-8674(92)90030-g.
5. Oettinger MA, Schatz DG, Gorka C, Baltimore D. RAG-1 and RAG-2, adjacent genes that synergistically activate V(D)J recombination. Science. 1990 Jun 22;248(4962):1517-23. doi: 10.1126/science.2360047.
6. Kassmeier MD, Mondal K, Palmer VL, Raval P, Kumar S, Perry GA, Anderson DK, Ciborowski P, Jackson S, Xiong Y, Swanson PC. VprBP binds full-length RAG1 and is required for B-cell development and V(D)J recombination fidelity. EMBO J. 2012 Feb 15;31(4):945–58. doi: 10.1038/emboj.2011.455. Epub 2011 Dec 13.
7. Wang L, Wuerffel R, Kenter AL. NF-kappa B binds to the immunoglobulin S gamma 3 region in vivo during class switch recombination. Eur J Immunol. 2006 Dec;36(12):3315–23. doi:10.1002/eji.200636294.
8. Yan M, Zhang X, Pu Q, Huang T, Xie Q, Wang Y, Li J, Wang Y, Gu H, Huang T, Li Z, Gu J. Immunoglobulin G Expression in Human Sperm and Possible Functional Significance. Sci Rep. 2016 Feb;1;6:20166. doi:10.1038/srep20166.
9. Wan X, Lei Y, Li Z, Wang J, Chen Z, McNutt M, Lin D, Zhao C, Jiang C, Li J, Pu Q, Su M, Wang Y, Gu J. Pancreatic Expression of Immunoglobulin G in Human Pancreatic Cancer and Associated Diabetes. Pancreas. 2015 Nov;44(8):1304-13. doi: 10.1097/MPA.0000000000000544. PMID: 26390427.
10. Lei Y, Huang T, Su M, Luo J, Korteweg C, Li J, Chen Z, Qiu Y, Liu X, Yan M, Wang Y, Gu J. Expression and distribution of immunoglobulin G in the normal liver, hepatocarcinoma and postpartial hepatectomy liver. Lab Invest. 2014 Nov;94(11):1283–95. doi: 10.1038/labinvest.2014.114. Epub 2014 Sep 29. PMID: 25264708.
11. Zhao Y, Liu Y, Chen Z, Korteweg C, Gu J. Immunoglobulin g (IgG) expression in human umbilical cord endothelial cells. J Histochem Cytochem. 2011 May;59(5):474 – 88. doi: 10.1369/0022155411400871. Epub 2011 Mar 23. PMID: 21430258; PMCID: PMC3201178.
12. Niu N, Zhang J, Sun Y, Wang S, Sun Y, Korteweg C, Gao W, Gu J. Expression and distribution of immunoglobulin G and its receptors in an immune privileged site: the eye. Cell Mol Life Sci. 2011 Jul;68(14):2481-92. doi: 10.1007/s00018-010-0572-7. PMID: 21061041.
13. Bronson R. Is the oocyte a non-professional phagocyte? Hum Reprod Update. 1998 Nov-Dec;4(6):763 – 75. doi: 10.1093/humupd/4.6.763. PMID: 10098468.
14. Taşdemir M, Ekiz-Yılmaz T, Uğur-Yılmaz C, Orhan N, Doğan MA, Arıcan N, Kaya M, Ahıshalı B. The effects of CLP-induced sepsis on proliferation and apoptosis of granulosa and theca cells in rat ovary: A histochemical and ultrastructural study. Reprod Biol. 2020 Sep;20(3):408–416. doi: 10.1016/j.repbio.2020.04.003. Epub 2020 May 20. PMID: 32444274.
15. Liu C, Su K, Tian M, Ji H, Sun L, Li C, Zhou X. Effects of three abnormal conditions of fallopian tube on outcomes of the in vitro fertilization and embryo transfer technique. J Obstet Gynaecol Res. 2020 Aug;46(8):1412–1418. doi: 10.1111/jog.14306. Epub 2020 Jun 4. PMID: 32500588.

16. Liu C, Su K, Tian M, Ji H, Sun L, Li C, Zhou X. Effects of three abnormal conditions of fallopian tube on outcomes of the in vitro fertilization and embryo transfer technique. J Obstet Gynaecol Res. 2020 Aug;46(8):1412–1418. doi: 10.1111/jog.14306. Epub 2020 Jun 4. PMID: 32500588.
17. Fillatreau S, Manfroi B, Dörner T. Toll-like receptor signalling in B cells during systemic lupus erythematosus. Nat Rev Rheumatol. 2021 Feb;17(2):98–108. doi:10.1038/s41584-020-00544-4. Epub 2020 Dec 18. PMID: 33339987; PMCID: PMC7747191.
18. Schweighoffer E, Nys J, Vanes L, Smithers N, Tybulewicz VLJ. TLR4 signals in B lymphocytes are transduced via the B cell antigen receptor and SYK. J Exp Med. 2017 May 1;214(5):1269–1280. doi: 10.1084/jem.20161117. Epub 2017 Mar 29. PMID: 28356391; PMCID: PMC5413329.
19. Das A, Heesters BA, Bialas A, O'Flynn J, Rifkin IR, Ochando J, Mittereder N, Carlesso G, Herbst R, Carroll MC. Follicular Dendritic Cell Activation by TLR Ligands Promotes Autoreactive B Cell Responses. Immunity. 2017 Jan 17;46(1):106–119. doi: 10.1016/j.immuni.2016.12.014. PMID: 28099860; PMCID: PMC8140609.
20. Schweighoffer E, Nys J, Vanes L, Smithers N, Tybulewicz VLJ. TLR4 signals in B lymphocytes are transduced via the B cell antigen receptor and SYK. J Exp Med. 2017 May 1;214(5):1269–1280. doi: 10.1084/jem.20161117. Epub 2017 Mar 29. PMID: 28356391; PMCID: PMC5413329.
21. Wang X, Zhang D, Sjölinder M, Wan Y, Sjölinder H. CD46 accelerates macrophage-mediated host susceptibility to meningococcal sepsis in a murine model. Eur J Immunol. 2017 Jan;47(1):119–30. doi:10.1002/eji.201646397. Epub 2016 Dec 21. PMID: 27794168.
22. Zhang J, Niu N, Wang M, McNutt MA, Zhang D, Zhang B, Lu S, Liu Y, Liu Z. Neuron-derived IgG protects dopaminergic neurons from insult by 6-OHDA and activates microglia through the FcγR I and TLR4 pathways. Int J Biochem Cell Biol. 2013 Aug;45(8):1911–20. doi: 10.1016/j.biocel.2013.06.005. Epub 2013 Jun 17. PMID: 23791745.
23. Kaya Z, Tretter T, Schlichting J, Leuschner F, Afanasyeva M, Katus HA, Rose NR. Complement receptors regulate lipopolysaccharide-induced T-cell stimulation. Immunology. 2005 Apr;114(4):493–8. doi: 10.1111/j.1365-2567.2004.02113.x. PMID: 15804286; PMCID: PMC1782106.
24. Gu Y, Liu Y, Fu L, Zhai L, Zhu J, Han Y, Jiang Y, Zhang Y, Zhang P, Jiang Z, Zhang X, Cao X. Tumor-educated B cells selectively promote breast cancer lymph node metastasis by HSPA4-targeting IgG. Nat Med. 2019 Feb;25(2):312–22. doi:10.1038/s41591-018-0309-y. Epub 2019 Jan 14. PMID: 30643287.
25. Satriano J, Schlondorff D. Activation and attenuation of transcription factor NF-kB in mouse glomerular mesangial cells in response to tumor necrosis factor-alpha, immunoglobulin G, and adenosine 3':5'-cyclic monophosphate. Evidence for involvement of reactive oxygen species. J Clin Invest. 1994 Oct;94(4):1629–36. doi: 10.1172/JCI117505. PMID: 7929839; PMCID: PMC295323.
26. Hill L, Ebert A, Jaritz M, Wutz G, Nagasaka K, Tagoh H, Kostanova-Poliakova D, Schindler K, Sun Q, Bönelt P, Fischer M, Peters JM, Busslinger M. Wapl repression by Pax5 promotes V gene recombination by Igh loop extrusion. Nature. 2020 Aug;584(7819):142–147. doi: 10.1038/s41586-020-2454-y. Epub 2020 Jul 1. PMID: 32612238; PMCID: PMC7116900.

27. Diwanji N, Bergmann A. Basement membrane damage by ROS- and JNK-mediated Mmp2 activation drives macrophage recruitment to overgrown tissue. Nat Commun. 2020 Jul 20;11(1):3631. doi: 10.1038/s41467-020-17399-8. PMID: 32686670; PMCID: PMC7371875.
28. Zhang YL, Guo YJ, Li B, Sun SH. Hepatitis C virus single-stranded RNA induces innate immunity via Toll-like receptor 7. J Hepatol. 2009 Jul;51(1):29–38. doi: 10.1016/j.jhep.2009.03.012. Epub 2009 Apr 17. PMID: 19443072.
29. Sioud M. Single-stranded small interfering RNA are more immunostimulatory than their double-stranded counterparts: a central role for 2'-hydroxyl uridines in immune responses. Eur J Immunol. 2006 May;36(5):1222-30. doi: 10.1002/eji.200535708. PMID: 16609928.

Figures

Figure 1

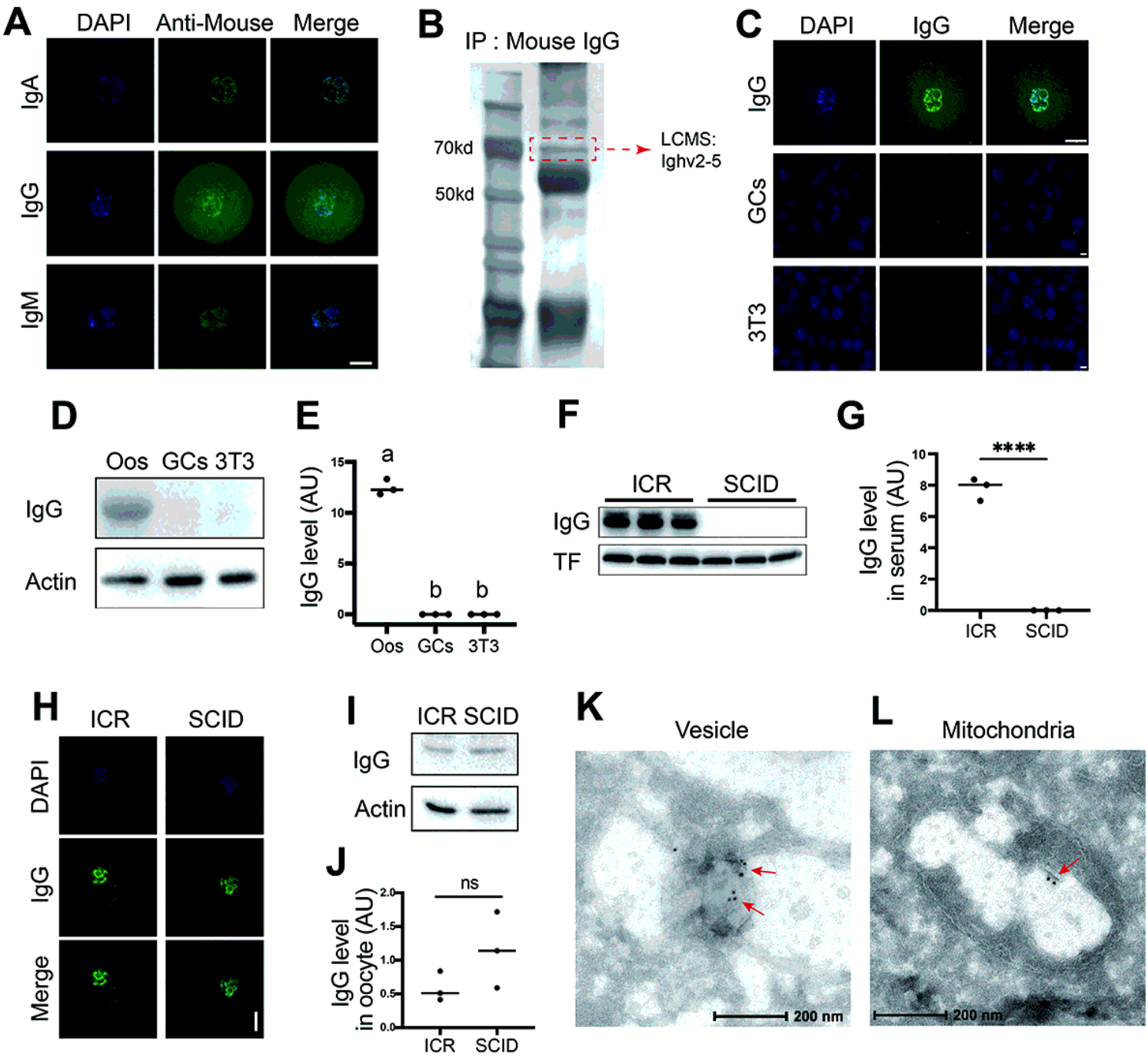

Figure 1

Immunoglobulins are present in oocytes

A. Immunofluorescence shows that different types of immunoglobulins, including immunoglobulin A (IgA), immunoglobulin G (IgG), and immunoglobulin G (IgM), are all present in mouse oocytes. B. Immunoprecipitation with anti-mouse IgG, SDS-PAGE, silver staining, and LCMS show that the right-size band, which corresponds to the size of the IgG (dot-line square labeled) includes Ighv2-5 (Blue-highlighted in supplementary dataset 1). C. Comparative immunofluorescence shows that IgG is rich in the oocytes

but is rarely seen in granular cells (GCs) or NTH3T3 (3T3) cells. D and E. Comparative Western blot and quantification show that IgG is rich in the oocytes but is not detectable in granular cells (GCs) or NTH3T3 (3T3) cells. F-J. Immunofluorescence and Western blot show that IgG is rich in the serum of the control mice but completely absent in the serum of the immunodeficient SCID (server combined immune-deficiency) mice (F and G); however, IgG levels in the control ICR oocytes and SCID oocytes are quite similar (H-J). K and L. Immuno-EM showed that IgG is present within diverse cytoplasmic organelles such as vesicle (K) and mitochondria (L). Actin or transferrin (TF) was used as a loading control. **** indicates p □ 0.0001.

Figure 2

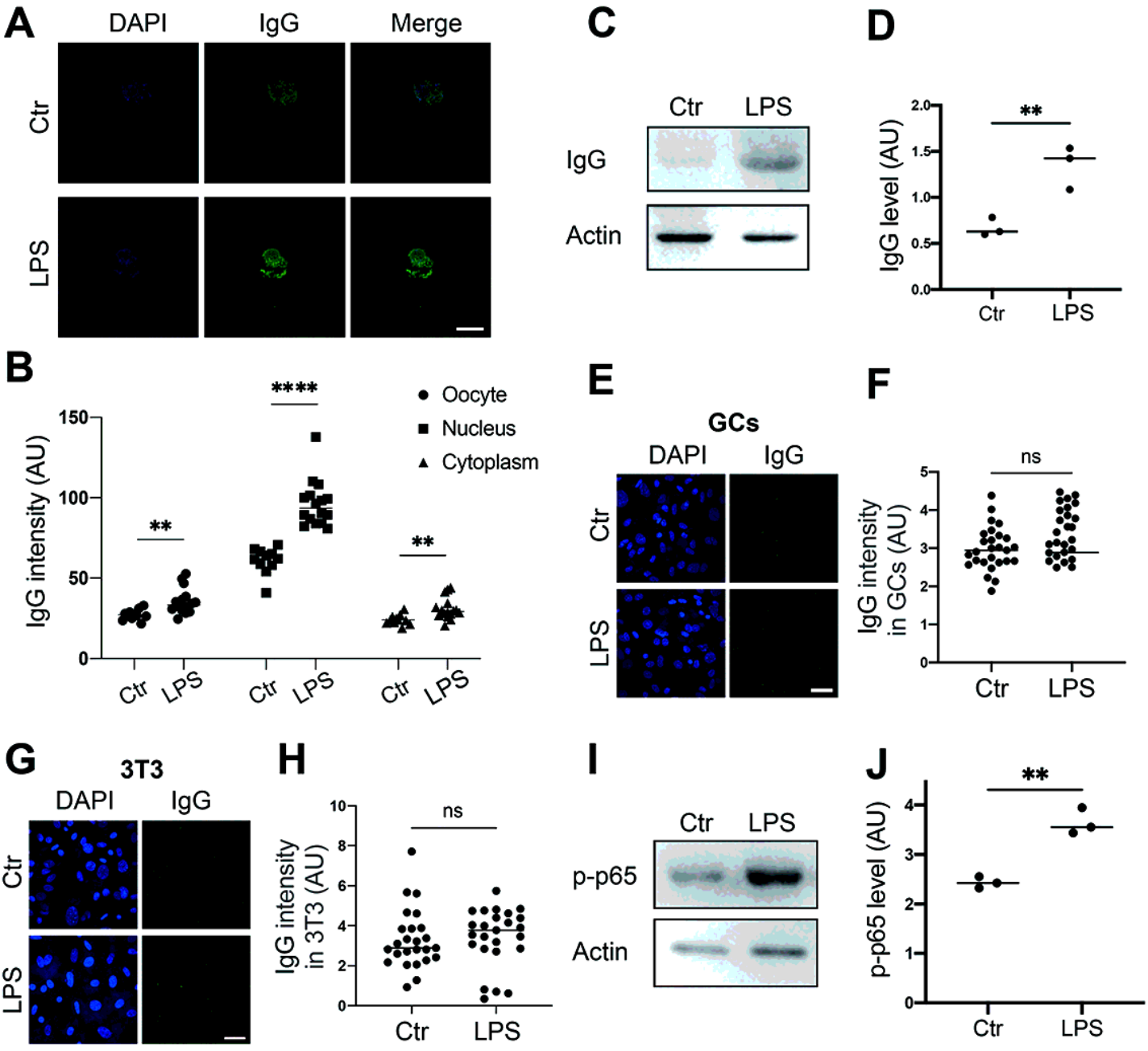

Figure 2

IgG protein increased in response to environmental LPS

A and B. Immunofluorescence shows that IgG increased more than one fold in response to LPS, and nuclear IgG increased more significantly. C and D. Western blot and quantification show that IgG protein level increased more than one fold in response to LPS (Lipopolysaccharide) supplemented in the IVM (in vitro maturation) medium. E-H. Immunofluorescence shows that IgG intensity is very low in control granular cells (GCs, E and F) or NIH3T3 (3T3s, G and H) and did not increase at all on exposure to LPS stimuli. I and J. Western blot and quantification show that p-NFKB (p-p65) significantly increased in response to LPS. Actin was used as a loading control. Actin was used as a loading control. ** indicates p 0.01. **** indicates p 0.0001.

Figure 3

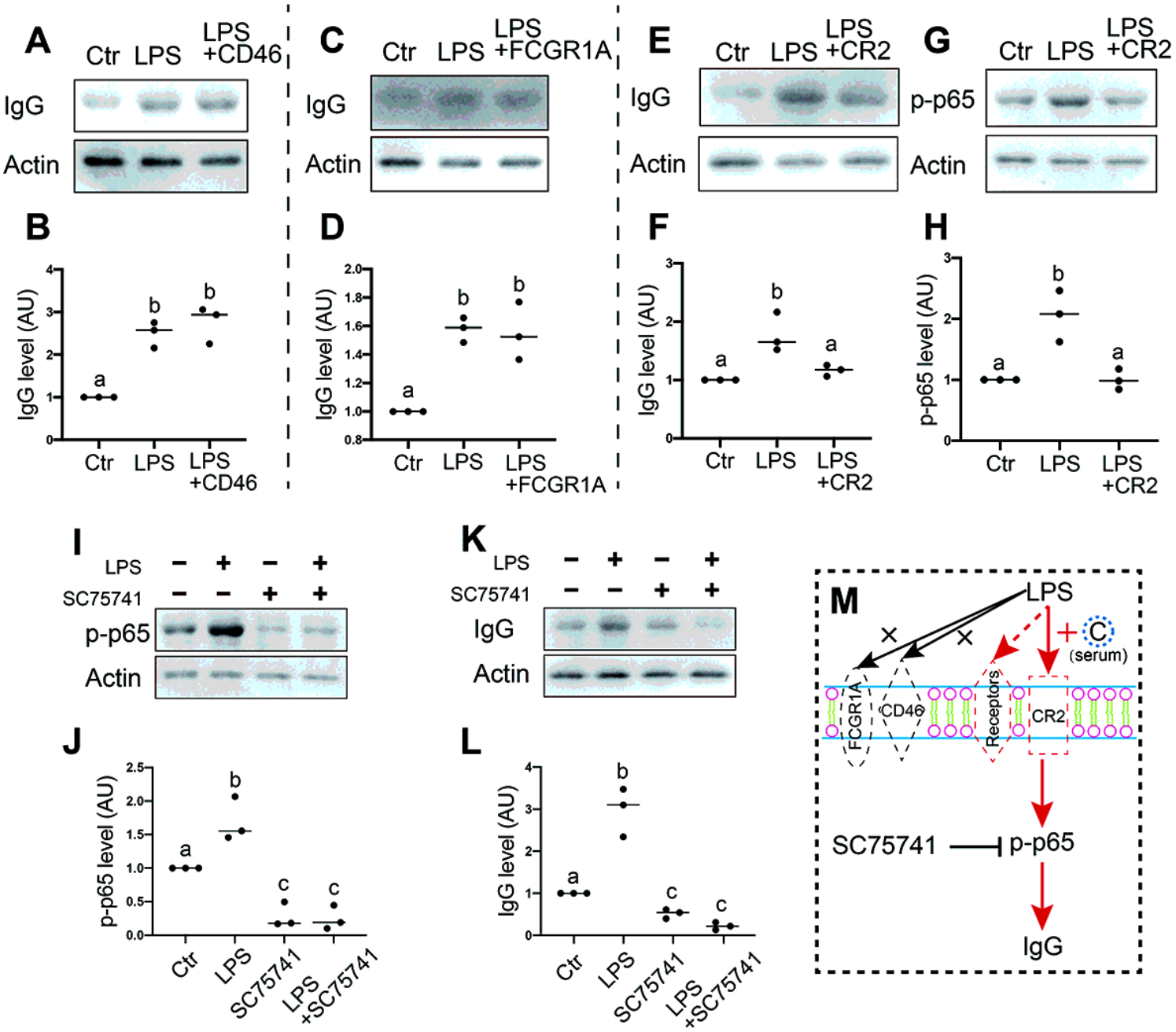

Figure 3

Membrane receptor CR2 mediates IgG production in response to environmental LPS

A and B. Western blot and quantification show that on exposure to LPS stimuli, IgG levels significantly increased about one fold, and CD46 (CD46 antigen, complement regulatory protein) blockage with the anti-CD46 antibody had no impact on the LPS-induced IgG increment. C and D. Western blot and quantification show that FCGR1A (Fc fragment of IgG receptor Ia) blockage with anti-FCGR1A antibody had no impact on the LPS-induced IgG increment. E-H. Western blot and quantification show that CR2 (complement receptor 2) blockage with anti-CR2 antibody brought the LPS-induced IgG increment back to

the control level (E and F). CR2 blockage also brought LPS-induced p-p65 increment back to the control level (G and H). I-L. Western blot and quantification show that on exposure to LPS stimuli, both p-p65 and IgG level significantly increased about one fold, and the NFKB inhibitor SC75741 brought the LPS-induced p-p65 or IgG increment back to the control level. M. Model hypothesis for A-L. LPS-induced increment of p-p65→IgG is mediated by membrane receptor CR2, not CD46 or FCGR1A. Actin was used as a loading control. Difference lower-case letters indicate significant difference between two groups.

Figure 4

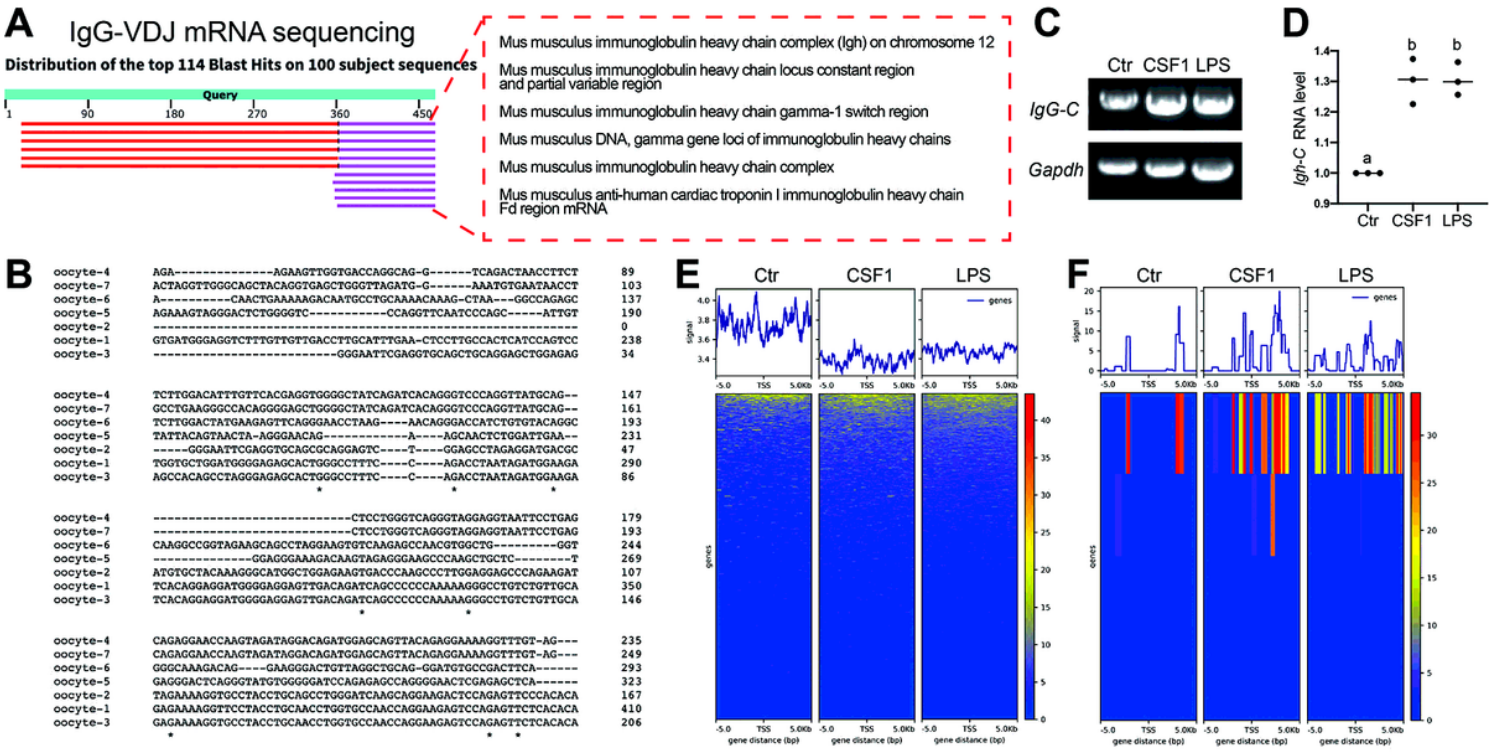

Figure 4

IgG transcription increased and was regulated by H3K27ac

A. Amplification of IgG-VDJ region, cloning and sequencing shows that IgG-VDJ mRNA is present in the oocyte. B. Parallel comparison of IgG-VDJ mRNA sequences from A. shows that IgG-VDJ mRNAs are highly distinct between different oocytes. C and D. Amplification of IgG constant (IgG-C) region showed that IgG-C mRNA levels significantly increased on exposure to either LPS or CSF1 stimuli. E and F. H3K27ac chip-seq showed that on exposure to either LPS or CSF1 stimuli, H3K27ac decreased its binding to the regulating sequences of all genes; however, its binding to the regulating sequences of the IgG gene significantly increased. *Gapdh* was used as a loading control. Difference lower-case letters indicate significant difference between two groups.

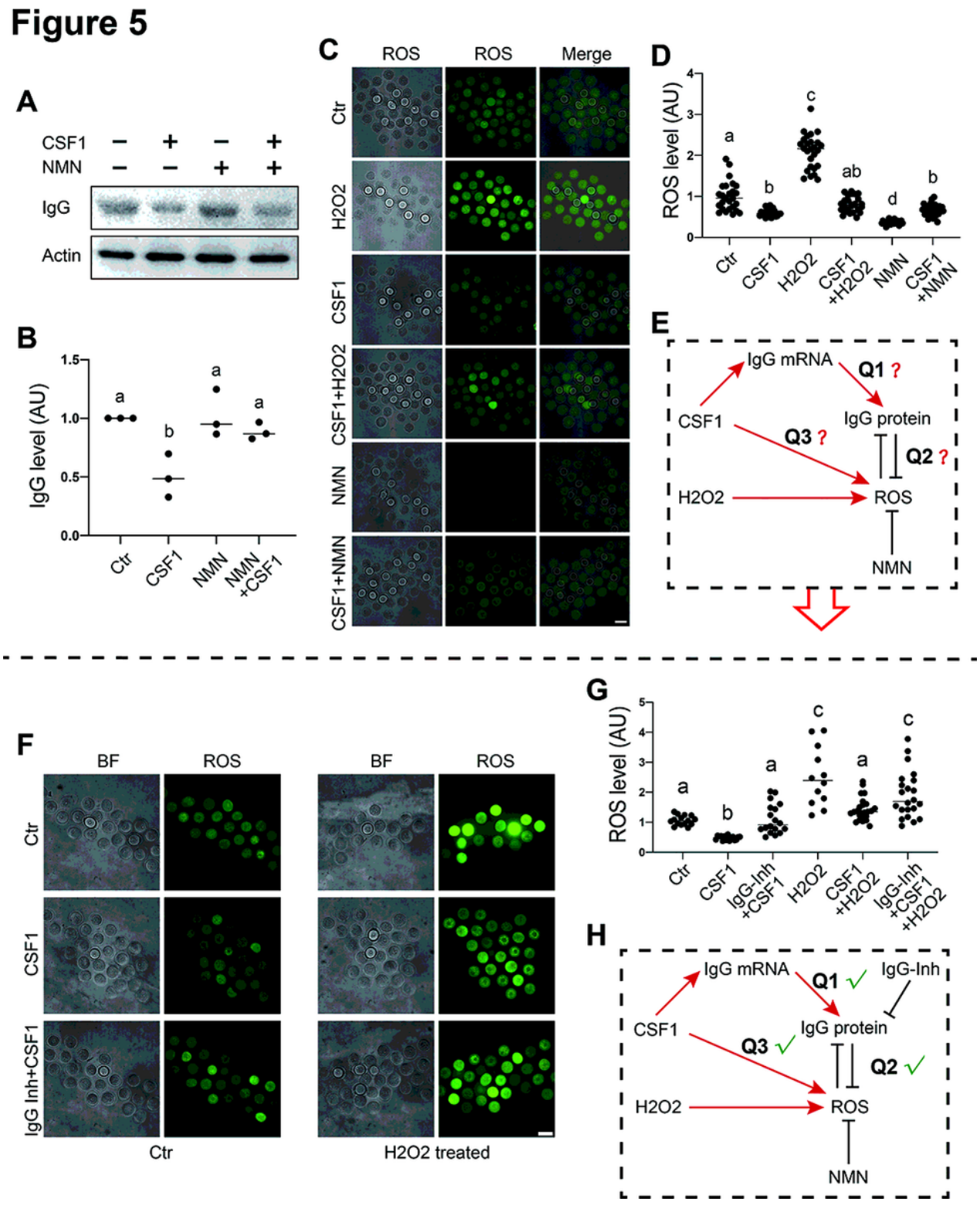

Figure 5

IgG functions to eliminate ROS production in response to CSF1 stimuli

A and B. Western blot and quantification show that on exposure to CSF1 stimuli, IgG levels significantly decreased about one fold. NMN supplement significantly raised the IgG level close to the control level. C and D. ROS live fluorescence shows that on exposure to CSF1 stimuli, ROS significantly decreased by

about 40.1%; on exposure to NMN supplement, ROS significantly decreased over one fold; on exposure to H2O2 stimuli, ROS significantly increased by more than one fold. CSF1 co-supplement with NMN raised the ROS level in NMN-treated oocytes to close to the control level; CSF1 co-supplement with H2O2 reduced the ROS level in H2O2-treated oocytes to near the control level. E. Model hypothesis for A-D. CSF1-induced IgG increment might be used to eliminate ROS production on exposure to either CSF1 or H2O2 treatment. F and G. ROS live fluorescence shows that on exposure to CSF1 stimuli, ROS significantly decreased by about 53.7%; while IgG co-inhibition significantly raised the ROS level close to the control level. On exposure to H2O2 stimuli, ROS significantly increased by more than one fold; the CSF1 co-supplement reduced the ROS level in H2O2-treated oocytes to close to the control, whereas IgG inhibition+CSF1+H2O2 significantly increased the ROS level compared with the CSF1+H2O2 group. H. Model hypothesis for A-G: CSF1 treatment could induce both IgG and ROS increment; increased IgG can be used to counteract the increment of ROS on exposure to CSF1 or H2O2 stimuli. Actin was used as a loading control. Difference lower-case letters indicate significant difference between two groups.

Figure 6

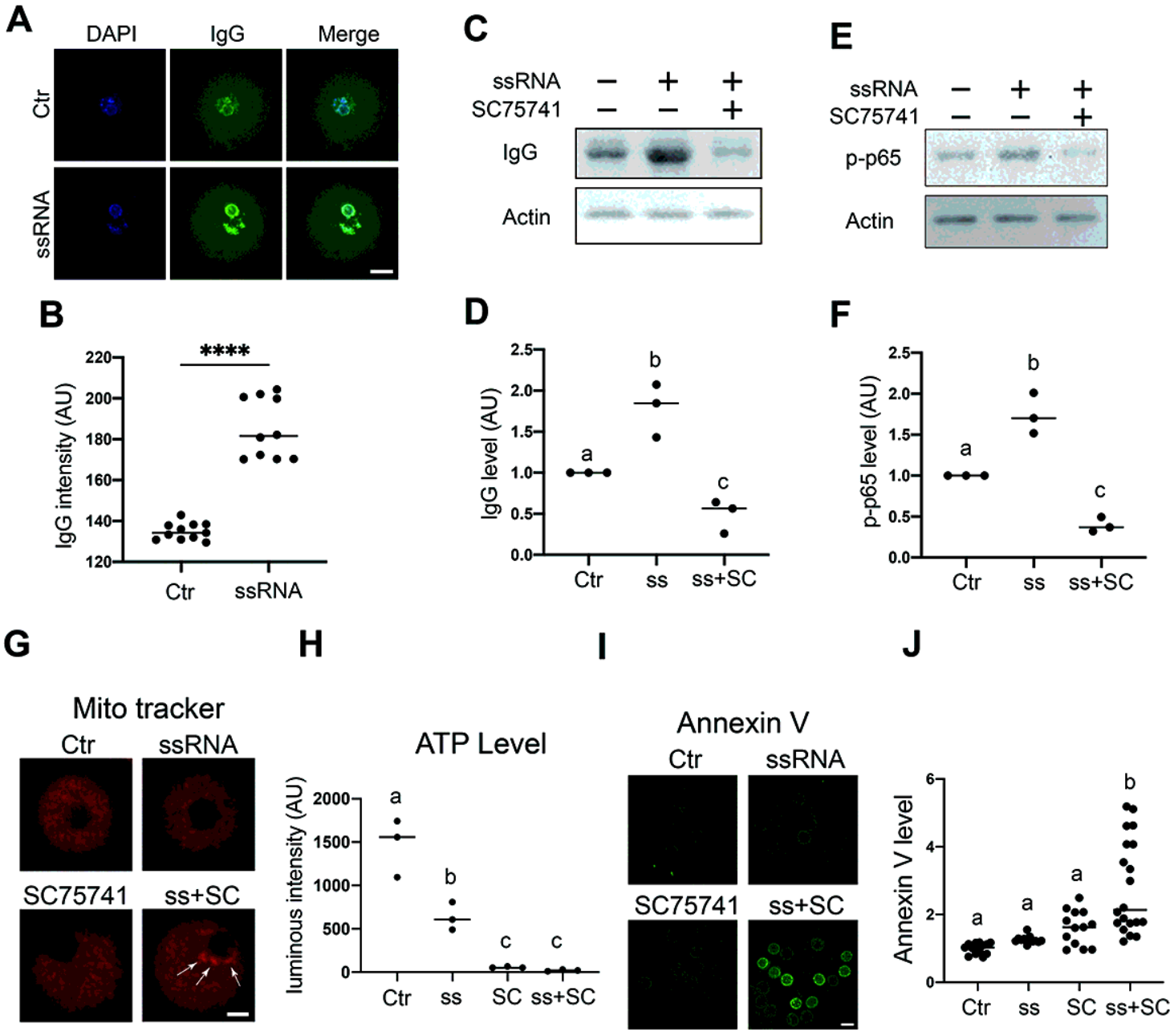

Figure 6

IgG functions to protect mitochondria integrity in response to virus ssRNA stimuli

A and B. Immunofluorescence shows that IgG intensity significantly increased in virus ssRNA-injected oocytes. DNA in blue, IgG in green. C-F. Western blot and quantification show that upon virus ssRNA injection, the IgG level significantly increased, whereas the NFKB inhibitor SC75741 significantly brought the ssRNA-induced IgG increment back to the control level. The p-p65 level also significantly increased upon ssRNA injection, whereas the SC75741 significantly brought the ssRNA-induced p-p65 increment back to the control level. G and H. Mitochondria live fluorescence showed that both ssRNA injection and NFKB inhibition caused increased mitochondria aggregation, accordingly ATP level significantly

decreased upon either treatment. While ssRNA injection combined with NFKB inhibition further exacerbate mitochondria aggregation, accordingly ATP level further decreased. I and J. Live fluorescence showed that early apoptotic level indicated by Annexin V significantly increased upon ssRNA injection combined with NFKB inhibition. Actin was used as a loading control. **** indicates p □ 0.0001. Difference lower-case letters indicate significant difference between two groups.

Figure 7

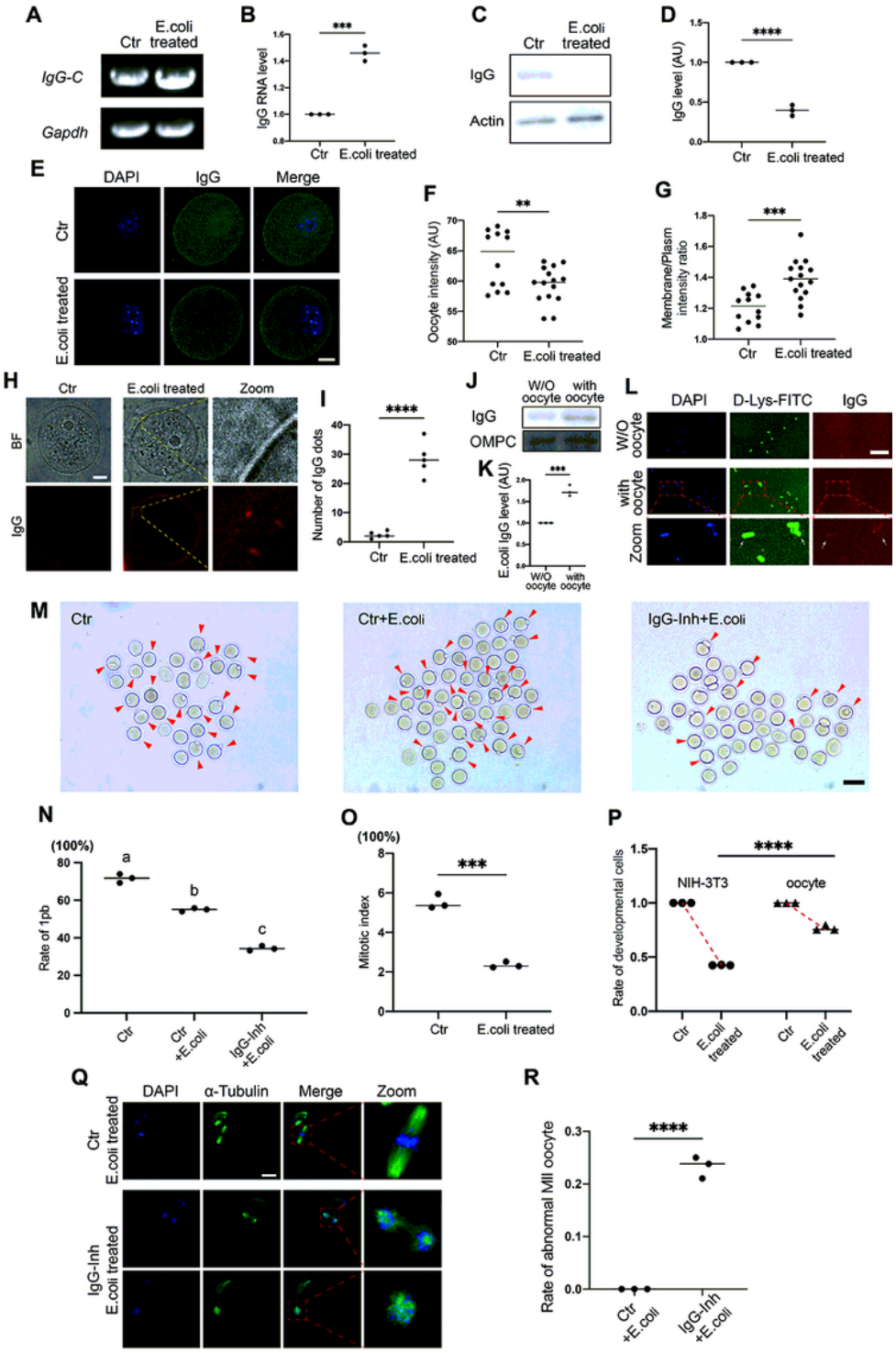

Figure 7

IgG functions to protect oocyte survival in response to E. coli stimuli

A-D. E. coli was added to the oocyte IVM medium. RT-PCR and quantification show that IgG-constant (IgG-C) mRNA level significantly increased on exposure to E. coli stimuli (A and B), whereas Western blot shows that IgG protein level significantly decreased (C and D). E-G. Immunofluorescence shows that on exposure to E. coli stimuli, IgG intensity within oocytes significantly decreased, however, the membrane/cytoplasm IgG ratio significantly increased. H and I. Live image of fluorescence dye (Cy2)-labeled IgG and quantification show that E. coli supplemented into the oocyte IVM medium caused increased IgG aggregates on the outside of the oocyte membrane. J and K. Western blot shows that after E. coli is supplemented into the oocyte IVM medium, the IgG protein level significantly increased in E. coli pellets. L. Immunofluorescence shows that E. coli supplemented into the oocyte IVM medium caused significantly increased IgG staining on E. coli. A region in oocyte-challenging E. coli was magnified and is shown below. DNA in blue, E. coli (D-Lys-FITC labeled) in green, IgG in red. M-P. IVM and quantification show that the mitosis and meiosis decrement extent of E. coli-challenged NIH3T3 (from 5.52% to 2.35%, O) was much larger than that of E. coli-challenged oocytes (from 71.65% to 55%, N). However, IgG inhibition further decreased the oocyte maturation rate from 55% to 34.4% (N). P. Side-by-side comparison of E-coli-treated NIH3T3 cells and oocytes showed that the decrement extent of the mitotic index was much larger than that of the oocyte maturation rate. Q and R. Immunofluorescence showed that IgG inhibition caused a significantly increased percentage of maturated oocytes with an abnormal chromosome alignment and spindle structure. *Gapdh,* Actin or OMPC (Escherichia coli Outer Membrane Pore Protein C) was used as a loading control. ** indicates p □ 0.01, *** indicates p □ 0.001. **** indicates p □ 0.0001. Difference lower-case letters indicate significant difference between two groups.

Supplementary Files

This is a list of supplementary files associated with this preprint. Click to download.

- SupplementaryFigure1.tif
- Supplementarydataset1.xlsx
- WangYetalSupplementaryinformation.docx